



HAL
open science

Self-similar concentration profiles in buoyant mixing of miscible fluids in a vertical tube

Marie Debacq, Vincent Fanguet, Jean-Pierre Hulin, Dominique Salin, Bernard Perrin

► **To cite this version:**

Marie Debacq, Vincent Fanguet, Jean-Pierre Hulin, Dominique Salin, Bernard Perrin. Self-similar concentration profiles in buoyant mixing of miscible fluids in a vertical tube. *Physics of Fluids*, 2001, 13 (11), pp.3097-3100. 10.1063/1.1405442 . hal-00984190

HAL Id: hal-00984190

<https://hal.science/hal-00984190>

Submitted on 27 Apr 2022

HAL is a multi-disciplinary open access archive for the deposit and dissemination of scientific research documents, whether they are published or not. The documents may come from teaching and research institutions in France or abroad, or from public or private research centers.

L'archive ouverte pluridisciplinaire **HAL**, est destinée au dépôt et à la diffusion de documents scientifiques de niveau recherche, publiés ou non, émanant des établissements d'enseignement et de recherche français ou étrangers, des laboratoires publics ou privés.

LETTERS

The purpose of this Letters section is to provide rapid dissemination of important new results in the fields regularly covered by *Physics of Fluids*. Results of extended research should not be presented as a series of letters in place of comprehensive articles. Letters cannot exceed four printed pages in length, including space allowed for title, figures, tables, references and an abstract limited to about 100 words. There is a three-month time limit, from date of receipt to acceptance, for processing Letter manuscripts. Authors must also submit a brief statement justifying rapid publication in the Letters section.

Self-similar concentration profiles in buoyant mixing of miscible fluids in a vertical tube

M. Debacq, V. Fanguet, J. P. Hulin,^{a)} and D. Salin

Laboratoire Fluides Automatique et Systèmes Thermiques, UMR 7608, CNRS, Universités P. et M. Curie and Paris Sud, Bâtiment 502, Campus Universitaire, 91405 Orsay Cedex, France

B. Perrin

Laboratoire de Physique de la Matière Condensée, UMR 8551, CNRS, Ecole Normale Supérieure, Département de Physique, 24 rue Lhomond, 75231 Paris Cedex 05, France

(Received 31 May 2001; accepted 26 July 2001)

The influence of the density contrast (characterized by the Atwood number At) on gravity-induced mixing between two miscible fluids in a long vertical tube has been studied experimentally. Cross-section averaged fluid concentration profiles along the tube are measured optically: for large enough At values, they display a self-similar dependence in a broad range of times and distances and verify a diffusion law with an effective diffusivity 10^5 times higher than for molecular diffusion. At lower At values, this diffusive domain is limited by a sharp front moving at a velocity increasing with At . Below a threshold At value the diffusive behavior disappears. © 2001 American Institute of Physics. [DOI: 10.1063/1.1405442]

Rayleigh–Taylor instabilities can develop when a dense fluid overlies a lighter one.^{1–6} We shall be concerned here with the case of miscible fluids which is relevant to many practical situations^{6–8} such as laser induced nuclear fusion, extraction columns or fire propagation in vertical shafts. Most studies have been devoted to the characterization of the growth of the mixing zone through the displacement of the average front. After initial transient regimes, it is often observed to be quadratic with time and then linear.^{9–12} Front displacement laws close to $t^{0.5}$ have been reported in vertical tubes for displacements larger than the tube diameter.^{7,8} Self-similar structures of Rayleigh–Taylor flows with characteristic lengths increasing as $t^{2/5}$ have also been predicted theoretically.¹³

The present Letter is focused on the study of self-similar concentration profiles created by buoyant mixing of two miscible fluids in a long vertical tube. In a previous study, Baird *et al.*⁷ analyzed the mixing of a volume of salt solution dropped at the top of a tube filled with water but the time dependence of the concentration profile was not identified. In addition to the observation of a front displacement law near $t^{0.5}$, Zukoski *et al.*⁸ measured, in the same setup, concentration profiles after this front had reached the end of the tube; these results were analyzed in terms of a turbulent diffusivity model. In our experiments, the interface is initially at mid-height; the concentration profiles are measured before the

mixing zone reaches either end of the tube ($\Delta t < 20$ min) which allows to neglect their influence. Above a threshold density contrast At_m , these profiles display a self-similar dependence on the ratio of distance and of the square root of time.

Experiments are realized in a 4 m high vertical perspex tube of internal diameter $d = 20$ mm with a sliding slot valve in the middle. The setup is illuminated from behind. The lighter fluid is water dyed with nigrosine (40 mg/l). The heavy fluid is a solution of water and CaCl_2 salt at a concentration between 0.05 and 300 g/l. Density contrasts are characterized by the Atwood number $At = (\rho_2 - \rho_1) / (\rho_2 + \rho_1)$ that varies from 2×10^{-5} to 10^{-1} (ρ_1 and ρ_2 are the densities of the two fluids and their viscosity is nearly equal to that of water). At the beginning of each experiment, the upper and lower halves of the tube are, respectively, filled with the heavy and light solutions. Mixing is initiated by opening the slot valve (which takes a few tenths of a second) and the typical duration of the measurements is 1200 s. A few test experiments were performed with zero or weakly stabilizing density contrasts: no significant mixing occurred for several hours. Otherwise, the Rayleigh numbers are always far above the threshold (67.8) for RT instabilities.^{2,3}

Figure 1 displays frames from video recordings at two different Atwood numbers close to the lower and upper limits of the studied range. At a low density contrast [$At = 8 \times 10^{-4}$, Figs. 1(a)–1(c)], the initial instability finger displays a mushroom shape characteristic of finite Reynolds numbers (10 or more). Transverse waves develop in the

^{a)} Author to whom correspondence should be addressed. Electronic mail: hulin@fast.u-psud.fr

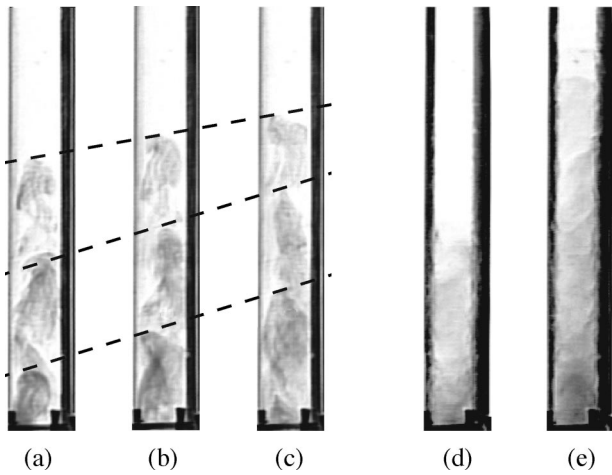


FIG. 1. (a)–(c) Video images obtained for $At=8 \times 10^{-4}$ at equal time intervals $\Delta t=2$ s. Height of field of view: 300 mm. The slot valve is visible at the bottom of the images. Dashed lines mark the trajectories of the front tip (upper line) and of concentration fluctuations moving inside the mixing zone (lower lines). (d)–(e) Video images obtained for $At=9 \times 10^{-2}$ at an interval $\Delta t=14$ s (same field of view).

wake of the finger which takes a helical shape.^{14,15} These features reflect instabilities due to the strong shear gradient at the interface between the ascending and descending fluids; they induce transverse mixing across the pipe and thus determine the final concentration profile. Two fluid patches of higher density contrast [darker color in Figs. 1(a)–1(c)] propagate in the wake of the leading tip and move faster than it. Their successive arrival at the front prevents the front speed to decrease through mixing with the surrounding fluid. At higher density contrasts $At \geq 5 \times 10^{-3}$, the initial instability finger is rapidly destroyed and the mixture is more homogeneous [Figs. 1(d) and 1(e)]. Fluid volumes of characteristic scale about 1 cm move randomly at velocities of the order of a few mm/s over distances of the order of the tube diameter: this flow is weakly turbulent and induces an efficient mixing similar to eddy diffusion.¹⁶ The displacement front is therefore quite fuzzy in the opposite of the well defined one at the lower Atwood number.

Quantitative results are obtained by recording with a digital camera images of a 2.6 m long central section of the tube (1300 × 20 pixels) at 2 s intervals. Using an independent

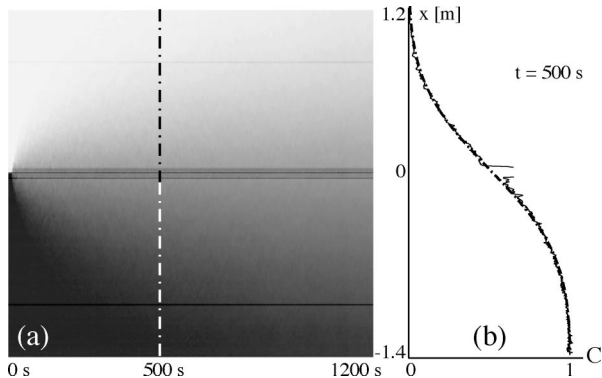


FIG. 2. Spatiotemporal diagram of normalized mean concentration $C(x,t)$ ($At=1.5 \times 10^{-2}$). Abscissa is time t and ordinate distance x from valve. (b) Normalized concentration profile $C(x,t=500$ s) fitted with an error function (dashed–dotted line).

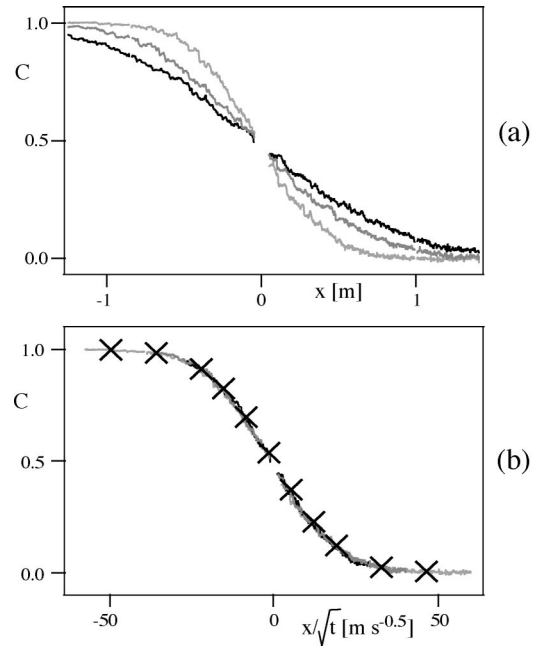


FIG. 3. (a) Variations of $C(x,t)$ with distance from valve at successive times ($t=240$ s, 600 s, and 1080 s) in the experiment of Fig. 2 ($At=1.5 \times 10^{-2}$). (b) Same curves as a function of x/\sqrt{t} . (×) Fit with an error function ($D=2.75 \times 10^{-4}$ m² s⁻¹).

calibration, these images are translated into concentration maps and normalized between reference images obtained with the heavy and light solutions. Finally, values corresponding to a same height x are averaged to obtain the instantaneous profile $C(x,t)$.

A typical result is shown in Fig. 2 at a high density contrast ($At=3.5 \times 10^{-2}$). The time dependence of the mixing process has been visualized by grouping the successive profiles into spatiotemporal diagrams [Fig. 2(a)]: gray levels correspond to the value of $C(x,t)$ (black for the dyed lighter solution, white for the transparent heavy one). Only a continuously varying gray shade is visible implying that the amplitude and size of relative concentration fluctuations are small [Figs. 1(d) and 1(e)]. No clear-cut boundary of the mixing zone is observed either. The concentration profiles at given times are well fitted by an error function as in Fig. 2(b) for $t=500$ s, which suggests that $C(x,t)$ verifies a diffusion equation. To test this hypothesis, concentration profiles obtained at different times in the same experiment [Fig. 3(a)] are plotted as a function of the scaling variable x/\sqrt{t} [Fig. 3(b)]. All curves collapse onto a single one $C(x/\sqrt{t})$: such fully self-similar sets of profiles are observed at all high Atwood numbers ($4 \times 10^{-3} \leq At \leq 10^{-1}$). Different scaling laws have been tested by plotting the profiles as a function of x/t^α . A good superposition is only obtained for $\alpha=0.5 \pm 0.03$. The fit of the profiles by error function solutions of a 1D diffusion equation provides an effective diffusivity D , which has thus a purely macroscopic meaning.

The behavior at lower Atwood numbers ($1.5 \times 10^{-4} \leq At \leq 2 \times 10^{-3}$) is different. In contrast with the previous case, the mixing region has a sharp boundary [Fig. 4(a)] associated to the tip of the finger in Figs. 1(a)–1(c) and marked by concentration steps (arrows) on the profiles of Figs. 4(b) and 5(a). The local slope of the boundary repre-

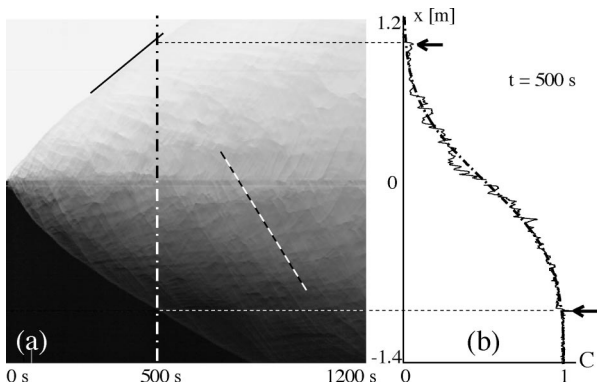


FIG. 4. (a) Spatiotemporal diagram of normalized concentration $C(x,t)$ ($At=4 \times 10^{-4}$). The slopes of the continuous and of the dashed lines correspond respectively to the instantaneous velocity V_t of the front tip and to the characteristic velocity V_f of the internal fluid motions. (b) Concentration profile $C(x,t=500\text{ s})$. Note concentration steps bounding the mixing zone (arrows).

sents the instantaneous velocity V_t of the tip of the displacement front. At low At values, V_t is roughly constant with time as in the linear regime found in other geometries.⁹ At higher density contrasts, V_t decreases with time [Fig. 4(a)] and the coordinate x_t of the tip varies approximately as $t^{0.5}$ as already observed by other authors.^{7,8} Note however that the typical front velocity V_t (measured at short times) increases, as expected physically, from 1 to 5 mm/s over the range of At values investigated.

However, in spite of these important differences between this regime and the previous one, all successive profiles of Fig. 5(a) still overlay as above when plotted as a function of the reduced variable x/\sqrt{t} [Fig. 5(b)]. This master curve is also well fitted by an error function in spite of the larger

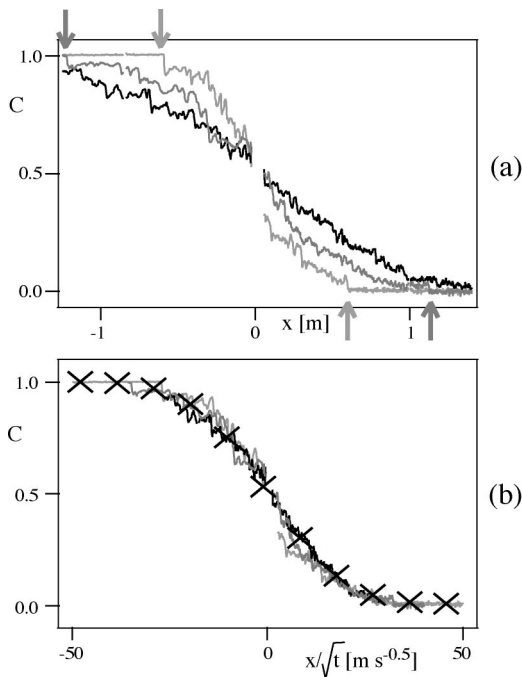


FIG. 5. (a) Variations of normalized concentration $C(x,t)$ with distance from valve at successive times ($t=240\text{ s}$, 600 s , and 1080 s) in the experiment of Fig. 4 ($At=4 \times 10^{-4}$). Note successive front positions indicated by arrows. (b) Same curves as a function of x/\sqrt{t} . (x) Fit with an error function ($D=2.5 \times 10^{-4}\text{ m}^2\text{ s}^{-1}$).

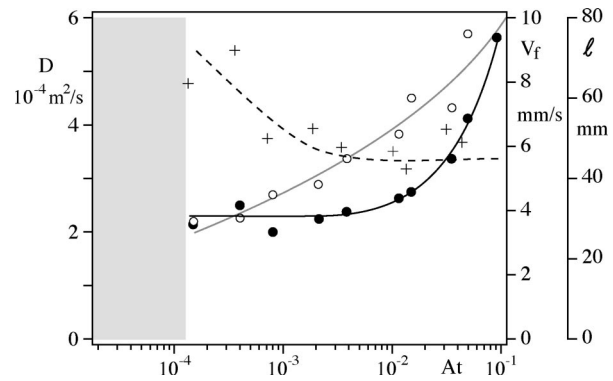


FIG. 6. Variation of the measured diffusivity D (●) and velocity V_f (○) with the Atwood number At . The characteristic length $\ell=D/V_f$ (+) is also plotted. The relative error on D is below 10% except for $At=1.5 \times 10^{-4}$ for which it is of the order of 30%. The gray zone at the left corresponds to At domain for which the spreading of the concentration profile is not diffusive.

fluctuations of the concentration values. The self-similar variation is however only followed between the concentration steps (except at long times where the profile can be considered as diffusive at all distances). This latter evolution towards a fully macroscopically diffusive regimes occurs later as At decreases. It is likely due to the influence of helical instabilities of the wake of the displacement fingers enhancing mixing across the pipe.

At still lower Atwood numbers ($At < At_m = 1.5 \times 10^{-4}$), the flow configuration is quite different. In particular, a stable counterflow of the two fluids is observed in the central part of the tube. Its length increases with time and helical instabilities persist then only near the ends of the tube. In this regime, the global concentration profiles cannot be fitted by error functions.

Variations of the macroscopic diffusivity D as a function of the Atwood number are displayed in Fig. 6. D is always at least 10^5 times larger than typical molecular diffusion coefficients (a few $10^{-9}\text{ m}^2\text{ s}^{-1}$). At lower At values ($At \leq 10^{-2}$) but above the threshold ($At_m = 1.5 \times 10^{-4}$), D is about constant and of the order of $2.5 \times 10^{-4}\text{ m}^2\text{ s}^{-1}$. At large At values ($At > 10^{-2}$), D increases roughly linearly with At from $2.5 \times 10^{-4}\text{ m}^2\text{ s}^{-1}$ to $6 \times 10^{-4}\text{ m}^2\text{ s}^{-1}$ (for $At=10^{-1}$).

Since the mixing and spreading of the two fluids is associated to internal fluid motions in the mixing zone, D may be considered as the product of their characteristic velocity V_f and a length ℓ . Such fluid motions are visible in Figs. 1(a)–1(c) and are marked by oblique streaks in the spatiotemporal diagrams [Fig. 4(a)]. V_f values determined from the slope of these streaks are plotted in Fig. 6: they increase slowly with At from 2 to 10 mm/s over the range studied. The variation of the characteristic length $\ell=D/V_f$ with At is also displayed in Fig. 6. From this point of view, the fact that D is roughly constant in the range $1.5 \times 10^{-4} \leq At \leq 10^{-2}$ results from variations of V_f and ℓ in opposite directions with At while retaining a constant product. For $At > 10^{-2}$, Fig. 6 indicates that ℓ reaches a lower limit of the order of 45 mm, probably related to the tube diameter: the increase of D with At , would then reflect that of V_f .

These experiments demonstrate that gravity induced mixing in long vertical tubes displays self-similar character-

istics down to Atwood numbers as low as $At_m = 1.5 \times 10^{-4}$: the average concentration $C(x,t)$ over the tube section depends only on x/\sqrt{t} and follows a diffusion law (at least in its central part). The corresponding coefficient D remains almost constant down to $At \approx At_m$ below which the flow pattern changes and the diffusive behavior disappears. This does not mean that, as the density contrast goes to zero, the growth rate of the mixing region does not vary: at low At values, it is determined by the motion of the tip of the displacement front at a velocity V_t which does decrease with the density contrast as expected. This tip represents a cutoff point beyond which the self-similar trend of the concentration profile is not followed any more.

The macroscopic diffusion coefficient D is determined by local relative motions of small fluid volumes of different concentrations. At high At values, the flow is weakly turbulent and the process is analogous to eddy diffusivity. At low density contrasts (although above At_m), transverse mixing by helical instabilities of the wake of the displacement front is a major factor of the appearance of a diffusive profile: these instabilities originate in the shear layers resulting from the counterflow of the two fluids. At still lower density contrasts ($At < At_m$) regions of stable counterflow appear and the profile is not any more diffusive. A full understanding of these mechanisms will require the study of the influence of the tube diameter as well as of the viscosity of the fluids involved, that we are now investigating.

ACKNOWLEDGMENTS

We thank G. Chauvin, M. Delisée, and C. Saurine who designed and realized the experimental setup, E. Lefaucheur and M. Souche for the realization of the preliminary experiments, J. Bush for a careful and constructive reading of the paper and A. Acrivos, P. Dimotakis, and E. J. Hinch for useful suggestions. We are grateful to G. Daccord and the SRPC–Schlumberger Center who initiated and funded this research.

- ¹Lord Rayleigh, "Investigation of the character of the equilibrium of an incompressible heavy fluid of variable density," Scientific Papers, ii, 200-7, Cambridge, GB, 1900.
- ²G. I. Taylor, "The instability of liquid surfaces when accelerated in a direction perpendicular to their planes," Proc. R. Soc. London, Ser. A **201**, 192 (1950).
- ³G. K. Batchelor and J. M. Nitsche, "Instability of stationary unbounded stratified fluid," J. Fluid Mech. **227**, 357 (1991); "Instability of stratified fluid in a vertical cylinder," *ibid.* **227**, 419 (1991).
- ⁴S. Chandrasekhar, *Hydrodynamic and Hydromagnetic Stability* (Oxford University Press, Oxford, 1961), and references therein.
- ⁵H.-J. Kull, "Theory of the Rayleigh–Taylor instability," Phys. Rep. **206**, 197 (1991).
- ⁶D. H. Sharp, "An overview of Rayleigh–Taylor instability," Physica D **12**, 3 (1984).
- ⁷M. H. I. Baird, K. Aravamudan, N. V. Rama Rao, J. Chadam, and A. P. Peirce, "Unsteady axial mixing by natural convection in vertical column," AIChE J. **38**, 1825 (1992).
- ⁸E. E. Zukoski, "A review of flows driven by natural convection in adiabatic shafts," NIST Report NIST-GCR-95-679, 1995, and references therein; J. B. Cannon and E. E. Zukoski, "Turbulent mixing in vertical shafts under conditions applicable to fires in high rise buildings," Technical Fire Report No. 1 to the National Science Foundation, California Institute of Technology, Pasadena, California, 1975.
- ⁹R. A. Wooding, "Growth of fingers at an unstable diffusing interface in a porous medium or Hele–Shaw cell," J. Fluid Mech. **39**, 477 (1969).
- ¹⁰S. B. Dalziel, P. F. Linden, and D. L. Young, "Self-similarity and internal structure of turbulence induced by Rayleigh–Taylor instability," J. Fluid Mech. **399**, 1 (1999), and references therein.
- ¹¹A. W. Cook and P. E. Dimotakis, "Transition stages of Rayleigh–Taylor instability between miscible fluids," J. Fluid Mech. **443**, 69 (2001).
- ¹²J. Fernandez, "Instabilités gravitationnelles entre fluides miscibles," thèse de doctorat, Pierre and Marie Curie University, Paris, France, 2000.
- ¹³N. A. Inogamov, A. M. Oparin, A. Y. Demy'anov, L. M. Dembitskioe, and V. A. Khokhlov, "On stochastic mixing caused by the Rayleigh Taylor instability," JETP **92**, 715 (2001).
- ¹⁴R. Bai, K. Chen, and D. D. Joseph, "Lubricated pipelining: stability of core-annular flow. Part 5. Experiments and comparison with theory," J. Fluid Mech. **240**, 97 (1992), and references therein.
- ¹⁵J. Scoffoni, E. Lajeunesse, and G. M. Homsy, "Interface instabilities during displacements of two miscible fluids in a vertical pipe," Phys. Fluids **13**, 553 (2001).
- ¹⁶G. I. Taylor, "Diffusion and mass transport in tubes," Proc. R. Soc. London, Ser. B **67**, 857 (1954).